Journal of Materials Chemistry B

Accepted Manuscript

ROYAL SOCIETY OF CHEMISTRY

www.rsc.org/materialsB

Cite this: DOI: 10.1039/c0xx00000x

www.rsc.org/xxxxxx

ARTICLE TYPE

Co-liposomes of Redox-Active Alkyl-Ferrocene Modified Low MW Branched PEI and DOPE for Efficacious Gene Delivery in Serum

Krishan Kumar,‡[a] Gururaja Vulugundam,‡[a] Paturu Kondaiah[b] and Santanu Bhattacharya*[a,c]

Received (in XXX, XXX) Xth XXXXXXXXX 20XX, Accepted Xth XXXXXXXXX 20XX

DOI: 10.1039/b000000x

Herein, we present six new lipopolymers based on low molecular weight, branched polyethylenimine (BPEI 800 Da) which are hydrophobically modified using ferrocene terminated alkyl tails of variable lengths. The effects of degree of grafting, spacer length and the redox state of ferrocene in the lipopolymer on the self assembly properties were investigated in detail by TEM, AFM, DLS and zeta potential measurements. The assemblies displayed an oxidation induced increase in the size of the aggregates. The co-liposomes comprising the lipopolymer and a helper lipid, 1,2-dioleoyl phosphatidyl ethanolamine (DOPE) showed excellent gene (*p*DNA) delivery capability in serum containing environment in two cancer cell lines (HeLa and U251 cells). Optimized formulations showed remarkably higher transfection activity than BPEI (25 KDa) and it was also significantly better than a commercial transfection reagent, Lipofectamine 2000 as evidenced from both the luciferase activity and EGFP expression analysis. Oxidation of ferrocene in lipopolymers led to drastically reduced levels of gene transfection which was substantiated by reduced cellular internalization of fluorescently labelled *p*DNA using confocal microscopy and flow cytometry. Moreover, the transfection inactive oxidized lipopolyplexes could be turned transfection active after their exposure to ascorbic acid (AA) in cell culture medium during transfection. Endocytosis inhibition experiments showed that gene expression mediated by reduced formulations involved both clathrin and caveolae mediated pathways while the oxidized formulations were routed via the caveolae. Cytotoxicity assay revealed no obvious toxicity for the lipopolyplexes in the range of optimized transfection levels in both the cell lines studied. Overall, we have exploited the redox activity of ferrocene in branched PEI based efficient polymeric gene carriers whose differential transfection activities could be harnessed for spatial or temporal cellular transfections.

Introduction

Last decade has witnessed an upsurge in developing non-viral vectors for gene therapy.[1-3] Their advantages include low immune response, inexpensive synthesis in large scale, and high flexibility regarding the delivery of larger sizes of genes, among others. Cationic polymers constitute an important class of vectors apart from cationic lipids in the category of non-viral gene delivery carriers.[4,5] Polymer-based carriers offer better advantages over liposomes owing to their higher stability, better buffering ability, small and narrow size distribution.[6] One or more desired properties can be achieved by altering their physicochemical parameters like chemical composition, molecular weight and structural design (linear, branched, block and graft copolymers). Popular prototypes in this category include polyethylenimine (PEI),[7-9] chitosan,[10] poly(l-lysine) (PLL), poly(2-N-(dimethylaminoethyl) methacrylate) (pDMAEMA), polyamidoamine dendrimers (pAMAM) and poly(α-[4-aminobutyl]-l-glycolic acid) (PAGA). Inspite of their promising features, most of them however, suffer from poor delivery efficiency and toxicity. Intense efforts are on to circumvent these drawbacks. Ever since Behr and co-workers demonstrated the gene delivery capability of polyethylenimines, this class of polymers has emerged as a potent candidate among the cationic polymers for gene delivery.[11] This is due to their inherent high cationic charge density and impressive proton sponge effect. Currently 25 kDa branched PEI and 22 kDa linear PEI are considered as benchmarks for the non-viral gene delivery. They effectively condense DNA into compact nano particles (polyplexes), the size of which is suitable for efficient cellular uptake via various endocytic pathways. After entering the cells, buffering action of amines allows their ready escape from endo-/lysosomal compartments.[11]

Even though high molecular weight PEIs (>25 kDa) show superior gene delivery efficacy, they are significantly cytotoxic and cause excessive cell death. These may be due to (i) the presence of large number of primary ammonium ions which adversely affect the cell membrane[12] and (ii) the formation of pores in mitochondrial membranes by internalized PEI.[13] On the other hand, low molecular weight PEI (<2 kDa) with low toxicity profiles display significantly lower transfection activity than 25

kDa BPEI.[14] Many investigators have accordingly embarked upon various modifications of low molecular weight PEI to improve transfection efficiency which include grafting of low molecular weight PEIs onto biocompatible polymers (e.g., dextran and chitosan),[15,16] hydrolytically or reductively degradable PEIs,[17-19] sugars,[20] and polyethylene glycol[21] etc. Hydrophobic modification of PEIs has displayed promising results as reflected from an increased physical encapsulation of genes and cellular uptake.[22,23] For instance, PEIs have been modified by alkyl chains of various lengths,[24,25] cholesterol,[26-28] phenyl boronic acid[29] and pluronic[30] etc.

Now the focus is on the design of drug and gene delivery systems which are sensitive to external stimuli like pH, ionic strength, light, temperature and redox potential where the delivery system is not merely a passive vehicle, but actively participates in the delivery.[31-34] Redox sensitivity is a common phenomenon in biological systems. Common strategies for reversible electron transfer to control the self-assembly process are generally achieved by employing disulfide bonds,[35] ferrocene,[36] tetrathiafulvalene,[37] and anthraquinones.[38] Ferrocene, an organometallic compound, is known for its redox properties and stability. In many cases, the oxidation state of ferrocene has been utilized to control the ability to deliver contents. Notably a ferrocene based cationic lipid, namely *bis*-(*n*-ferrocenyl-alkyl)dimethyl ammonium bromide (BFDMA), was used earlier to achieve relatively higher transfection levels in the reduced state of ferrocene while in the oxidized state it became substantially inefficient.[39, 40] Microcapsules constructed from a redox-sensitive poly(ferrocenylsilane) (PFS) allowed penetration of dextran after oxidation.[41] Yuan *et al* showed the release of rhodamine B dye which was encapsulated in poly(ethylene oxide)–ferrocene /poly(styrene)–β-cyclodextrin vesicles after oxidation of ferrocene.[42] Ferrocene grafted high molecular weight PEIs were also developed as amperometric biosensors[43], biofuel cells[44] and co-delivery of drug/DNA.[45] However, the corresponding ferrocene based lipopolymers with non-toxic low molecular weight BPEI have not been exploited for gene delivery.

We have previously reported excellent serum compatibility and efficient gene delivery by lipopolymers with variable grafting of cholesterol units on three different low molecular weight BPEIs.[28] Their interaction with 1,2-dipalmitoyl phosphatidyl choline (DPPC), a model phospholipid was also studied.[46] In this work we have introduced hydrophobic modification into the low molecular weight BPEI (800 Da) using long alkyl chained ferrocene for efficient redox controlled gene delivery. The ferrocene moieties were kept distant from the PEI backbone using variable lengths of hydrocarbon tethers, *i.e.*, six and eleven methylene units. Moreover, we have varied the percentage of hydrophobic modification to various extents into these polymers. The ferrocene terminated alkyl tails of variable length on the side chains of BPEI not only act as redox responsive triggers, but also contribute to the hydrophobicity of the resultant polymer. All the redox polymers formed aggregates in water which undergo an increase in their size upon application of the redox stimuli. The co-liposomes formed from the optimized ratio of redox polymers and 1,2-dioleoyl phosphatidyl ethanolamine (DOPE) show efficient gene delivery even in the presence of serum. Furthermore, we show their ability to deliver DNA to be dependent on the redox state of the ferrocenylated polymer and their cellular uptake route leading to gene expression. Additionally it may be further emphasized here that these formulations have the potential to deliver DNA on a 'demand' basis if the transfection activities of the oxidized lipoplexes which were almost transfection inactive, could be resumed in extracellular environments by means of a redox stimulus. We used ascorbic acid (AA) in cell culture medium during transfection of oxidized lipopolyplexes where a significant resumption was observed in gene expression levels. This is an extra beneficial tool which such systems could elicit for site specific and time regulated cellular transfections.[40,47] Thus, differential transfection activities of these lipopolymeric formulations could be useful for efficient cellular transfections as well as for transfections needed to be performed spatially or temporally under the influence of redox control.

Experimental

Materials and Methods

All reagents and solvents used in the present study were of highest grade commercially available and all were used purified, dried, or freshly distilled, as required. Starting materials, such as ferrocene, 6-bromohexanoic acid, 11-bromoundecanoic acid, anhydrous aluminium chloride, sodium borohydride and branched polyethylenimine (BPEI, average M_w= 800 Da and 25 kDa) were purchased from Sigma-Aldrich. 1,2-Dioleoyl-*sn*-glycero-3-phosphatidylethanolamine (DOPE) was purchased from Avanti Polar Lipids. Dubelcco's modified Eagle's medium (DMEM), Dulbeco's phosphate buffered saline (DPBS), thiazolyl blue tetrazolium bromide (MTT), chlorpromazine hydrochloride (CPZ), filipin and amiloride hydrochloride were obtained from Sigma. Fetal bovine serum (FBS) was obtained from Gibco. Luciferase assay kit was procured from Promega. Column chromatography was performed using a 60-120 mesh silica gel. IR spectra were recorded using Bruker FT-IR spectrometer. NMR spectra were recorded using a Bruker spectrometer (400 MHz for ^{1}H NMR and 100 MHz for ^{13}C NMR). The chemical shifts (δ) are reported in ppm downfield from the internal standard: TMS, for ^{1}H-NMR and ^{13}C-NMR. Mass spectra were recorded on a MicroMass ESI-TOF spectrometer. All the compounds were adjudged pure by ^{1}H NMR, ^{13}C NMR and mass spectroscopy.

Synthesis.

(6-Bromohexanoyl) ferrocene (**1**). To a solution of 6-bromohexanoic acid (3 g, 11.3 mmol) in 20 mL $CHCl_3$, 3 mL $SOCl_2$ was added dropwise for 15 min and then the mixture was refluxed for 6h. Excess thionyl chloride was removed under reduced pressure to give the crude 6-bromohexanoyl chloride. The crude compound was dissolved in 50 mL dry $CHCl_3$ and added dropwise over a period of 1h to a mixture of ferrocene (2.5 g, 13.6 mmol) and anhydrous $AlCl_3$ (1.8 g, 13.6 mmol) in dry $CHCl_3$ and stirred overnight under argon. The reaction was quenched by carefully adding ice-cold water dropwise. The organic portion was separated, extracted into $CHCl_3$, washed with brine, dried over anhydrous Na_2SO_4 and then dried under vacuum. Pure compound was obtained by column chromatography over silica gel using hexanes:ethyl acetate (15:85) as a reddish-orange solid.

(6-Bromohexanoyl) ferrocene[48] **(1)**: Yield 70%, ^{1}H NMR (400

MHz, $CDCl_3$) δ 4.78 (s, 2H), 4.50 (d, 2H), 4.20 (s, 5H), 3.45 (t, 2H, *J* = 6.8 Hz), 2.73 (t, 2H, *J* =7.2 Hz). ^{13}C NMR ($CDCl_3$, 100 MHz): *δ* (ppm) 204.0, 78.9, 72.1, 69.7, 69.2, 38.3, 33.7, 32.6, 28.0, 23.5 HRMS calcd. for [$C_{16}H_{19}BrFeO+Na^+$] 385.0070, found 385.0068.

(11-Bromoundecanoyl) ferrocene[49] **(2)**: Same procedure as described above was followed. Yield 75%, ^1H NMR (400 MHz, $CDCl_3$): δ 4.78 (d, 2H, *J* = 4.8 Hz), 4.50 (d, 2H, *J* = 4.8 Hz), 4.10 (s, 5H), 3.40 (t, 2H, *J* = 6.9 Hz), 2.62 (t, 2H, *J* = 7.5 Hz), 1.84 (m, 2H, *J* = 7.2 Hz), 1.68 (m, 2H) and 1.32 (m, 12H). ^{13}C NMR ($CDCl_3$, 100 MHz): *δ* (ppm) 205, 89.4, 68.6, 68.1, 67.1, 34.0, 32.8, 30.9, 29.5, 28.7, 28.0 HRMS calcd. for [$C_{21}H_{29}BrFeO+Na^+$] 455.0649, found 455.0649.

(6-Bromohexyl) ferrocene[48] **(3):** To a mixture of $NaBH_4$ (1.5 g, 39.2 mmol) and anhyd. $AlCl_3$ (2.6 g, 19.6 mmol) in dry THF was added a solution of **1** (3.6 g, 9.8 mmol) in dry THF dropwise over 1h while stirring vigorously under argon atmosphere. After stirring for 5h, reaction was quenched by dropwise addition of ice-cold water (20 mL). Organic layer was separated, extracted with $CHCl_3$, washed twice with water, brine and dried over anhydrous Na_2SO_4 and finally dried under vacuum. Pure compound was obtained by column chromatography over silica gel using hexanes:ethyl acetate (20:1) as a yellowish-orange solid. Yield 80%.

^1H NMR (400 MHz, $CDCl_3$) δ 4.10 (s, 5H), 4.05 (s, 4H), 3.41 (t, 2H), 2.32 (t, 2H), 1.86 (t, 2H), 1.47 (m, 4H), 1.34 (m, 2H). ^{13}C NMR ($CDCl_3$, 100 MHz): *δ* (ppm) 89.2, 68.4, 68, 67, 34, 32.8, 30.9, 29.5, 28.7, 28 HRMS calcd. for $C_{16}H_{21}BrFe$ 347.9297 (M^+), found 347.9291 (M^+).

(11-Bromoundecyl) ferrocene[49] **(4)**: Yield: 80%. ^1H NMR (400 MHz, $CDCl_3$) δ 4.20 (m, 9H), 3.41(t, 2H), 2.24 (t, 2H), 1.86 (m, 2H), 1.45 (m, 4H), 1.28 (m, 12 H). ^{13}C NMR ($CDCl_3$, 100 MHz): *δ* (ppm) 28.1, 28.7, 29.3, 29.4, 29.6, 31.0, 32.7, 34.0, 66.8, 67.9, 68.3, 89.4. HRMS calcd. for $C_{21}H_{31}BrFe$ 418.0959 (M^+), found 418.0955 (M^+).

Lipopolymer Synthesis

A slight modification of the report by Schmidtke *et al.* was adopted here for the lipopolymer synthesis.[50] Briefly, (6-bromohexyl) ferrocene (**2**) (0.5 g, 1.4 mmol) was dissolved in dry ethyl acetate and appropriate amount of PEI dissolved in dry methanol was added along with 5 eq of K_2CO_3. The reaction mixture was refluxed till TLC showed disappearance of (**2**). The reaction mixture was evaporated under vacuum and the residue was repetitively washed with hexane to remove residual ferrocenyl impurities. Then the residue was dissolved in $CHCl_3$ and filtered to remove any salts followed by drying under vacuum. This was subjected to extensive dialysis against deionized water (MW cut off: 7000) for 2 days followed by freeze drying. An analysis on precoated silica gel TLC plate using the product thus obtained showed the presence of a homogenously pure material at R_f ~0.2 ($CHCl_3$/MeOH/NH_4OH 70:28:2). All the lipopolymers were characterized by IR, ^1H NMR, ^{13}C NMR and ESI-MS.

Lipopolymers obtained upon treatment with 11-bromoundecyl ferrocene were synthesized in a similar procedure.

Degree of ferrocene grafting in PEI

The extent of ferrocene grafted on to each polymer was determined from ^1H NMR spectra as described by Schmidtke *et al*.[50] For this purpose, area under the peak for hydrogens of ferrocene moiety (δ 4.0-4.3) was set as standard and the remaining peaks were integrated relatively. PEI backbone has four non-exchangeable hydrogens in its repeat unit (–CH_2-CH_2-NH). The broad peak manifested in the region δ 2.2-3.0 (ΔA_{pei}) is due to the backbone –*CH_2-CH_2-N* of PEI as well as –*CH_2*– from the –*CH_2*-$(CH_2)_{n-1}$–Fc which are now attached to the PEI backbone. These two hydrogens are then subtracted from ΔA_{pei} to obtain the actual area of PEI backbone. The % grafting of alkyl ferrocene in each of the lipopolymer was calculated from:

% ferrocene grafting = $4/(\Delta A_{pei} - 2) \times 100$.

Sample Preparation[28]

Each of the redox lipopolymer alone or in combination with a desired amount of helper lipid, DOPE (w/w) were taken in a wheaton glass vial and dissolved in dry chloroform. A thin film was formed by drying the organic solvent under a steady stream of dry nitrogen which was then hydrated with an appropriate quantity of water or aqueous buffer at 4 °C. The suspensions containing redox lipopolymer alone were bath sonicated at 50 °C while the mixed suspensions of lipopolymer and DOPE were first subjected to a freeze-thaw cycle treatment (3 cycles) followed by bath sonication. Each of the suspensions was oxidized by adding ferric chloride (1.5 equiv., w/w) and vortexing for 5 min. For each of the further experiments freshly prepared oxidized co-liposomes were used.

Transmission Electron Microscopy (TEM)

The suspensions of the redox lipopolymers were examined using transmission electron microscopy with negative staining using 0.5% uranyl acetate. A 10 µL sample of the suspension was loaded onto Formvar coated, 400 mesh copper grids and allowed to remain for 5 min. Excess fluid was removed from the grids by touching their edges with filter paper, and 10 µL of 0.5% uranyl acetate was applied on the same grid after which the excess stain was similarly wicked off. The grid was vacuum-dried for 4 h, and the specimens were observed under TEM (JEOL 200-CX) operating at an acceleration voltage of 120 keV.

Atomic Force Microscopy (AFM)

AFM images were recorded on an atomic force microscope (AFM, JPK NanoWizard) by tapping mode in air. The aqueous suspensions were prepared as described above and deposited onto freshly cleaved mica. Immobilization was achieved using electrostatic forces between the opposed charges of the mica and polymeric suspensions. The sample was dried for 4 h under vacuum before measurement.

UV-Vis Absorption Spectroscopy

UV-Vis absorption spectra of the lipopolymer suspensions in the aqueous media were recorded using Shimadzu UV-2100 spectrophotometer at 25 °C.

Dynamic Light Scattering (DLS) & Zeta Potential Measurements

Hydrodynamic size and zeta potential of the aqueous suspensions of each of the lipopolymers alone and their respective mixtures with DOPE were measured using Zetasizer Nano ZS (Malvern Instruments, Malvern, UK) equipped with a He-Ne laser of 532 nm wavelength. The scattered light is detected at 173° (back scattering technique), amplified and analyzed by a correlator. The resulting correlation function is then analyzed by the software provided by the manufacturer to obtain a mean diameter.

The zeta potential was obtained by Laser Doppler

Velocimetry. The electrophoretic mobility was measured with a technique called M3-PALS (Phase analysis Light Scattering), from which the ζ-potential is extracted by using the Smoluchowski equation.[51] The measurements were performed in five independent replicates. The particle size and zeta potential measurements were also performed for the polyplexes which were prepared by addition of appropriate volume of lipopolymer/DOPE suspensions to 3 μg of plasmid DNA (*p*DNA).[52] They were incubated for 30 min and then diluted to 1 mL by adding mili-Q water prior to the measurements. In these measurements, the viscosity of the dilute lipopolymer suspensions was assumed to be same as that of water.

Gel Retardation Assay

To assess the DNA binding efficiency of the redox lipopolymeric conjugates, lipopolyplexes were prepared by adding each formulation to a constant amount of plasmid DNA (0.2 μg) to achieve the desired lipopolymer/*p*DNA w/w ratio such that the final volume is 20 μL. The lipopolyplexes were incubated for 30 min at room temperature and electrophoresis (100 V) was performed on 1% agarose gel for ~45 min. The images were recorded in a Gel Documentation System.

Cell Culture

HeLa and U251 cell lines were cultured in Dulbecco's modified Eagle's medium (DMEM) containing 10% fetal bovine serum (FBS) and antibiotic, pen strep (100 units/ml penicillin and 100 μg/ml streptomycin). Cells were incubated in a humidified atmosphere (relative humidity > 95%) with a CO_2 level of 5% at 37 °C. Trypsinization of cells at proper confluency using 0.5 % trypsin–EDTA was followed for passaging of cells at regular intervals.

Lipopolyplex Preparation

The plasmid DNA (pGL3 control or pEGFP-C3 plasmid, 0.4 μg) was complexed with reduced or oxidized lipopolymeric formulations (stock, 0.5 mg/mL) at five different w/w ratios (1:1 to 5:1) in cell culture medium, DMEM (100 μL). The complexation was allowed for a time period of 30 min. These complexes were added to the wells while maintaining different serum concentrations for transfection.

Luciferase Assay

Transfection studies were first performed in HeLa (human epithelial cervical carcinoma cell line) cells for the optimization of efficient formulations and then U251 (human glioma cell line) cells were also undertaken for transfection experiments. 24-well cell culture plates were seeded at the density of 40000 cells per well and allowed to grow for next 24 h. On the day of transfection, the old medium was removed from wells and washed twice with DPBS (Dulbecco's Phosphate-Buffered Saline) and 20% FBS containing DMEM (100 μL) was added. Polyplexes prepared as discussed above in DMEM were added to wells maintaining 10% serum condition (+FBS) for transfection experiments and incubated for 4 h at 37 ºC. Then old medium was removed, washed three times with DPBS and 10% FBS containing DMEM was added and incubation was continued for another 20 h. At this point old medium was removed, wells were washed properly with DPBS and cell lysis was performed by adding 100 μl of passive lysis buffer (Promega) to each well. The plate was kept on shaker for 30 min. The luciferase activity of samples was determined by using manufacturer's protocol with a luminometer. After checking luciferase activity, the protein concentration in samples was obtained using BSA protein assay kit (Bio-Rad) and results were represented as RLU/mg of protein. Triplicates for each w/w ratio were taken into consideration in transfection experiments and results were expressed based on at least 3 such independent experiments. The treatment of oxidized lipopolyplexes with ascorbic acid (10:1, ascorbic acid/lipid molar ratio) was done in cell culture medium during transfection experiments.

EGFP Expression Studies

pEGFP-C3 plasmid was used to check transfection levels of redox lipopolymer-lipid complexes in terms of GFP expression. After performing transfection as discussed above, cells were washed properly with DPBS and trypsinized using 0.5 % trypsin-EDTA. Cells were collected in 5% FBS containing DPBS and samples were then analysed using FACS Calibur flow cytometer (Becton-Dickinson). The data analysis was done using WinMDI 2.9 software and transfection level was expressed in terms of both % cells showing EGFP fluorescence and the intensity of fluorescence (Mean fluorescence intensity). For visual expression of EGFP levels, a fluorescence microscope (Olympus) was used.

Confocal Microscopy

To visualize the intracellular delivery of labelled *p*DNA (cy-5) using different lipopolymeric formulations, cells were cultured on cover slips placed in 12-well cell culture plates. Transfection was performed using 1 μg of DNA with lipopolymer formulation at w/w ratio of optimized transfection efficiency. After the transfection experiment, cells were washed with DPBS buffer three times and fixed in 4% paraformaldehyde solution for 10 min. Cells were then rinsed again with DPBS buffer thrice and treated with 0.1% triton-X-100 for 5 min to permeabilize the cell membrane. After a proper wash again with DPBS buffer, cells were kept for blocking in DPBS containing 10% fetal bovine serum for 1 h. Finally, the glass cover slips were taken out and treated with Hoechst 33342 for 5 min to counterstain the nucleus. Then the cells were washed properly with autoclaved milli-Q water and DPBS to remove excess dye and control overstaining. Finally the cover slips were mounted on glass slides and viewed under confocal laser scanning microscope (LSM meta, Zeiss).

In Vitro Cytotoxicity

Cytotoxicity of all the lipopolyplexes was evaluated in HeLa and U251 cell lines by conventional MTT assay.[53,54] In a typical experiment, cells were seeded at the density 10000 cells/well in a 96 well microplate. After 24 h cells were incubated with lipopolyplexes in 10% FBS containing DMEM (200 μL) following factual transfection conditions at different w/w ratios for a period of 4 h. Lipopolyplex incubation was then followed by replacing with 200 μl of fresh 10% FBS containing medium and incubating for another 16 h. At the end, each well was treated with MTT (20 μL, 5 mg/ml in DPBS) and incubated for 4 h. The experiment was terminated by removing whole medium from the wells, DMSO (200 μL) was added and absorbance was read at 570 nm on a microplate reader. Each experiment was performed in triplicates for each w/w ratio. The results expressed here are from at least three such independent experiments.

Endocytosis Inhibition

In a typical experiment, cells were pre-treated with chlorpromazine (5 μg/ml) or filipin (1 μg/ml) or amiloride (25 μg/ml) for about 30 min before transfection experiments started. The lipopolyplexes were added to the wells and allowed to

incubate for 2 h. The analysis for labelled *p*DNA cellular internalization experiments was made using FACS (Flow assisted cell sorting) and gene transfection levels using luciferase assay.

Statistical Analysis

The statistical analysis was performed based on the results of triplicate treatments from at least three independent experiments using student's t-test. The data were expressed with significance levels as $*P < 0.05$, $**P < 0.01$ and $***P < 0.001$.

Results and discussion

In this study we have hydrophobically modified low molecular weight branched polyethylenimines with ferrocene terminated alkyl tails. Thus, ferrocene redox centers were kept away from the PEI backbone by using two different lengths of hydrocarbon tethers containing six and eleven methylene units each. Additionally, we have varied the percentage grafting of ferrocene to various extents (Table S1, ESI†). The precursors, *n*-bromoalkyl ferrocene were prepared following a published procedure.[49] The modified redox-polymers, *P8-C6-Fx* and *P8-C11-Fx* (x = 1, 2 and 3) were synthesized by alkylation of the PEI amino groups using *n*-bromoalkyl ferrocene as shown in Scheme 1. Each of the modified polymers was characterized by IR, ^{1}H NMR, ^{13}C NMR and ESI-MS (Fig. S1-S4, ESI†). The % grafting was calculated as described in the experimental section. Here, P8- and -C6/C11 in the notation represent BPEI 800 Da and the spacer length respectively. Each of the two alkyl ferrocene tethers was grafted on BPEI to achieve three different degrees of substitution: low, medium and high represented as F1 (~15%), F2 (~25%) and F3 (~50%) respectively.

Scheme 1[a]

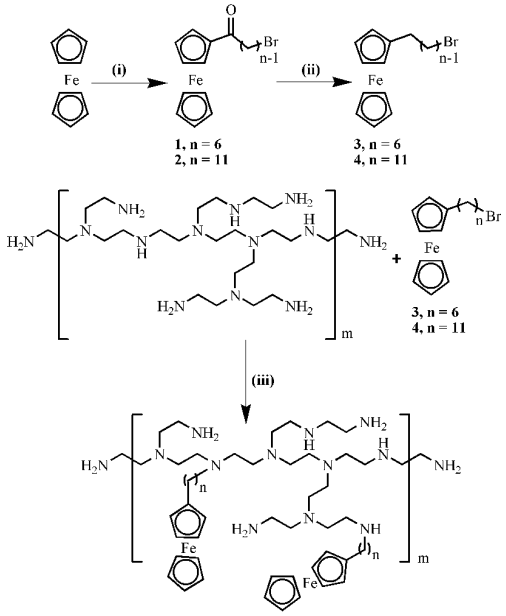

[a] Synthetic route to the ferrocene modified 0.8 kDa branched poly(ethyleneimine). (i) ω-alkanoyl chloride, anhyd. $AlCl_3$, CH_2Cl_2, RT, 12 h; (ii) $NaBH_4/AlCl_3$, THF, RT, 4 h; (iii) MeOH-EtOAc, K_2CO_3 reflux, 24 h.

All the ferrocene-grafted BPEI lipopolymers could be easily dispersed in aqueous medium and were stable for over at least one month. Aqueous suspensions of lipopolymer containing high grafting of ferrocene with eleven methylene units (P8-C11-F3) was slightly yellow and opalescent while those with lower percent grafting of both six and eleven methylene units afforded clear yellow suspensions readily. The yellow color of the lipopolymeric suspensions (1 mg/mL) was due to the presence of Fe (II) in the reduced state of ferrocene which was reflected as its characteristic absorption peak at 450 nm. Treatment of each polymeric suspension with $FeCl_3$ (1.5 equiv.) afforded the corresponding oxidized form, where the ferrocene moiety in the lipopolymer was transformed to a ferrocenium moiety as evidenced in its absorption spectrum as a new peak at 630 nm (Fig. S5, ESI†).

The size and morphology of these neat lipopolymer suspensions in aqueous media were first studied using atomic force microscopy (AFM) and transmission electron microscopy (TEM). In their unoxidized state, the lipopolymers, P8-C6-F1 and P8-C11-F1 showed the presence of nearly spherical structures in the range of 50-100 nm. Upon oxidation, we observed a clear increase in the sizes of the aggregates (140-200 nm). Representative AFM images of lipopolymeric aggregates are shown in Fig. 1A-D. The aggregates were further visualized under transmission electron microscope after negative staining using uranyl acetate (Fig. S6, ESI†) which confirmed the results obtained by AFM analysis where the size of the lipopolymeric aggregates increased from 40-80 nm to 110-200 nm when they were subjected to oxidation.

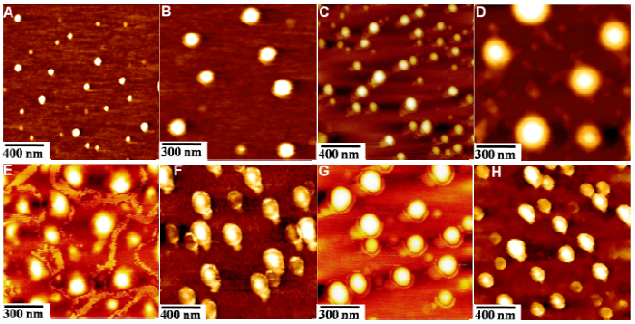

Fig. 1 Representative AFM images of redox lipopolymers alone (A-D) and gene transfection optimized co-liposomes of redox lipopolymers/DOPE (E-H) before (A, C, E and G) and after (B, D, F and H) oxidation. (DOPE:P8-C6-F1, 2:1 and DOPE:P8-C11-F1, 1.5:1)

In order to gain further insight about the effect of percentage ferrocene grafting as well as the oxidation state of the redox lipopolymer on the aggregate size, we characterized the aqueous suspensions of each lipopolymer by dynamic light scattering (DLS) technique (Table S1, ESI†). We observed that in the case of the unoxidized P8-C6-Fx series, the size of the lipopolymer aggregates increased with increasing extent of ferrocene grafting which followed the order as P8-C6-F1<P8-C6-F2<P8-C6-F3. Similar trend was seen in the case of the P8-C11-Fx series too. Additionally, the size of the aggregates increased as we moved from -C6 spacer to -C11 spacer. This may be because grafting of PEI with longer-alkylated ferrocene side-chains rendered it more hydrophobic than the one with shorter-alkylated ferrocene. This

could have also resulted in the formation of less compact aggregates. Interestingly, these aggregates showed changes in size as a consequence of redox reaction. Upon oxidation of these redox polymeric suspensions, there was a general increase in their size (Table S1 and Figure S7, ESI†). We believe that this is due to the electrostatic repulsion between the positively charged ferrocenium moieties that are present in the hydrophobic core of the aggregates. This presumably leads to the swelling of the core. Thus a change in the redox state of ferrocene moiety triggers transition in the size of the polymeric aggregates.

We also measured the zeta potential of the neat lipopolymeric suspensions which is a measure of the net surface charge density around the particle (Table S1). For the lipopolymers with ferrocene moiety in its native reduced state, we observed that the zeta potential of the aggregates decreased with increasing alkyl ferrocene grafting for both the P8-C6-Fx and P8-C11-Fx series. Also, the zeta potential decreased as we moved from P8-C6-Fx series to P8-C11-Fx series. This may be attributed to the hydrophobicity effect. In general, there was an increase in zeta potential of all the lipopolymer aggregates after oxidation, which is very much expected due to the formation of ferrocenium ions on the polymer backbone. For the oxidized suspensions, the effect of grafting on the polymer showed a different trend depending on the alkyl spacer length. Increasing the % alkyl ferrocene grafting led to reduction in the zeta potential for P8-C6-Fx series while for P8-C11-Fx series we found an increase in the zeta potential. This might be because, in P8-C11-Fx series, where ferrocene tethered via a longer alkyl chain -$(CH_2)_{11}$, upon oxidation, the positively charged ferrocenium moiety may loop towards the outer periphery of the micelle-like structures formed owing to its polar nature. With increasing grafting of the ferrocene terminated alkyl chains, this effect was more pronounced resulting in increased zeta potential.

It may be noted that the sizes of the aggregates as determined from the DLS studies are larger than that determined by TEM and AFM. This discrepancy in size characteristics between the two methods is probably because DLS technique measures the aggregates in their fully hydrated state while the TEM and AFM require the samples to be dried prior to the TEM or AFM recording. The drying induced reduction in sizes of other aggregates have been also reported.[36,55]

Then we proceeded to study the transfection optimized co-liposomes comprising lipopolymers and a neutral helper lipid, DOPE. The atomic force microscopic analysis evidenced presence of spherical morphology for both the reduced and oxidized states of the ferrocenylated lipopolymer (Fig. 1E-H). The sizes of the co-liposomal aggregates increased upon oxidation of the ferrocene moiety. While the unoxidized co-liposomes were of the size ~130-150 nm, oxidation enlarged their sizes to ~220-260 nm. Similarly, investigation of the co-liposomal suspensions using TEM (Fig. S8, ESI†) corroborated the observations of AFM where the size of co-liposomes of reduced state (110-150 nm) increased upon oxidation (200-250 nm).

Characterization of Lipopolymer-DOPE/*p*DNA Complexes

The complexes of optimized co-liposomes (lipopolymer and DOPE) with *p*DNA were characterized using AFM, DLS, zeta potential measurements and gel electrophoresis. AFM measurements revealed that the reduced forms of the co-liposomal formulations formed lipopolyplexes of uniform size and near-spherical shape (Fig. 2A and 2C), whereas their oxidized counterparts formed less compact and irregular structures of much larger size (Fig. 2B and 2D).

The particle sizes measured using DLS are shown in Fig. 2E. The lipopolymer:*p*DNA w/w ratio used to form complexes was a significant determinant of the hydrodynamic size. At lower w/w ratios (0.5 to 2), the sizes of the complexes formed were generally larger and similar to the complexes formed from the native BPEI (800 Da). Suspensions of P8-C6-F1 and P8-C11-F1 in their reduced form were able to condense plasmid DNA into nano-sized particles of diameter ~200 nm at w/w ratios of 3 to 5 while the unmodified BPEI (800 Da) formed larger particles. The influence of oxidation of ferrocene was clearly evident in the size of the polyplexes. The oxidized lipopolymeric formulations gave rise to larger sized complexes (~400 nm) than their reduced counterparts as supported by AFM studies.

Zeta potential measurements (Fig. 2F) showed that there was a significant impact of alkyl ferrocene substitution as well as the oxidation state of the ferrocene moiety. The complexes of the unmodified BPEI (800 Da) afforded zeta potentials ranging from slightly negative to weakly positive values. After the modification, P8-C6-F1 and P8-C11-F1 showed significantly positive zeta potential values (+20 to 30 mV) from w/w = 3. After oxidation, both the redox lipopolymers showed strongly positive zeta potential values.

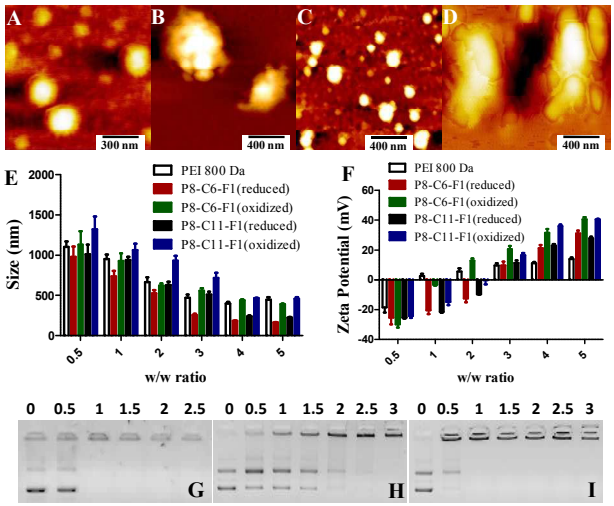

Fig. 2 Representative AFM images of lipopolyplexes (lipopolymer:*p*DNA, 4:1) of P8-C6-F1(A, B) and P8-C11-F1(C, D) in reduced (A, C) and oxidized (B, D) state. Particle sizes (E) and Zeta potentials (F) of lipopolyplexes prepared at different w/w ratios. Error bars are standard deviations of three independent measurements. Representative gel patterns for *p*DNA (0.2 µg) binding capability of native BPEI (800 Da) (G) P8-C6-F1 co-liposomes before (H) and after (I) oxidation. The numbers above each lane represent lipopolymer:*p*DNA (w/w) ratios.

The co-liposomal suspensions of the redox lipopolymers were complexed with *p*DNA at various w/w ratios ranging from 0.5:1 to 3:1 (lipopolymer/*p*DNA) and run on 1% agarose gel. It was observed that the native BPEI (800 Da) was able to retard *p*DNA

completely at w/w ratio of 1:1. However, the co-liposomes of lipopolymeric formulations showed slightly impaired *p*DNA binding ability. Oxidation of the lipopolymers led to drastic increase in the *p*DNA binding ability. The representative gel electrophoretic patterns for P8-C6-F1 in comparison with native BPEI (800 Da) are shown in Fig. 2G-I. The reduced P8-C6-F1 fomulation showed complete pDNA retardation at w/w 3:1 while its oxidized counterpart could retard pDNA completely at w/w 1:1 only. It should be noted that upon oxidation, the concomitant increase in the cationic charge density in the core of the aggregates might disturb the hydrophobic packing forming larger complexes (DLS studies) even though they are able to bind *p*DNA completely.

Gene Transfection Biology

The gene transfection activity of the ferrocene modified redox polymeric conjugates were first evaluated in HeLa (human epithelial cervical carcinoma) cells in 10% serum (FBS, fetal bovine serum) condition by luciferase assay and FACS (Flow Assisted Cell Sorting) analysis. Subsequently, transfection efficacies of optimized formulations were also carried out in U251 (Human glioma) cells. In HeLa cells, all the polymeric conjugates afforded substantial levels of gene expression where P8-C6-F1, P8-C6-F2 and P8-C6-F3 showed ~230, ~170 and ~80-fold increase respectively, when compared to native BPEI (800 Da) whereas P8-C11-F1, P8-C11-F2 and P8-C11-F3 afforded ~180, ~50 and ~30-fold increase respectively (Fig. S9, ESI†). However, the gene transfection levels afforded by the modified polymers were still lower than the 'gold standard' BPEI (25 kDa) (Fig. S9, ESI†). At this juncture, to augment the gene transfer capability of the redox polymeric conjugates, a well known helper lipid DOPE, was admixtured with the ferrocenylated polymeric conjugates.[28,56] The hydrophobic groups on PEI facilitated an easy integration into the lipid bilayer. Inclusion of DOPE gave rise to formulations with transfection capability significantly higher than BPEI (25 kDa) and even better than the potent commercially available reagent, Lipofectamine 2000, as described below.

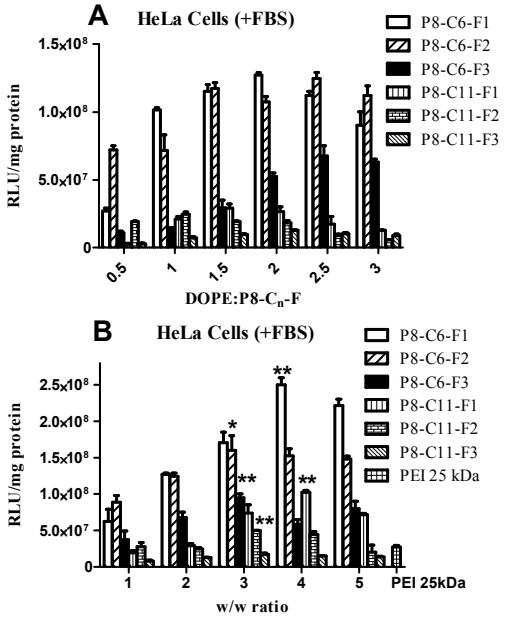

Fig. 3 Optimization of DOPE concentration in lipopolymer formulations while performing transfections at a fixed lipopolymer:DNA (w/w, 2) ratio (A) and maximum luciferase activities obtained from transfection of optimized formulations (B). Transfections were conducted using pGL3-control pDNA (0.4 μg) in 10% serum while using BPEI (25 KDa) as a positive control. The luciferase activities were examined for statistical significance in comparison with BPEI (25 KDa) (*$P < 0.05$ and **$P < 0.01$, Two-tailed Student's t-test).

Optimization of DOPE/Lipopolymer Ratio

DOPE was formulated with redox polymeric conjugates at w/w ratios ranging from 0.5:1 to 3.5:1. Each formulation was used in transfection experiments at w/w ratio of 2 with respect to *p*DNA (0.4 μg). The lipopolymers P8-C6-F1, P8-C6-F2 and P8-C6-F3 showed maximum transfection efficiency at DOPE:lipopolymer ratio of 2.0, 2.5 and 2.5 respectively (Fig. 3A). On the other hand, lipopolymers P8-C11-F1, P8-C11-F2 and P8-C11-F3 required lower amount of DOPE and elicited maximum transfection efficiency at DOPE:lipopolymer ratio of 1.5, 1.0 and 2.0 respectively (Fig. 3A). We observed that the transfection efficacies decreased with increasing grafting of alkyl ferrocene in both the series. Formulations containing the polymeric conjugates with shorter alkyl chain (C6) had relatively higher transfection efficiency than those with longer alkyl chain (C11).

Optimization of the Lipopolymer/DNA (w/w) ratio

Once the DOPE/lipopolymer ratios for each of the lipopolymer were optimized, each redox lipopolymer was tested by taking identical amount of *p*DNA (0.4 μg) and varying the amount of lipopolymer using the respective optimized lipopolymer/DOPE ratio at five (1:1 to 5:1) different lipopolymer/*p*DNA (w/w) ratios. Transfection efficacies for lipopolymers P8-C6-F1, P8-C6-F2, P8-C6-F3 remained significantly higher for all the five ratios studied compared to the BPEI (25 kDa) as evidenced from both luciferase assay (Fig. 3B) and FACS analysis (Fig. 4A and 4B).

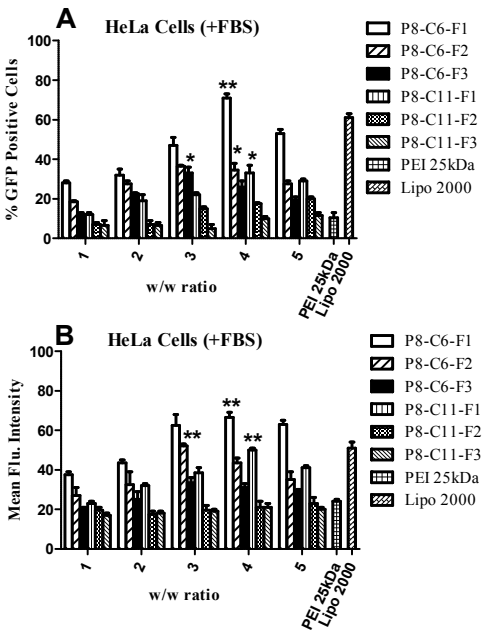

Fig. 4 Flow cytometry analysis of GFP expression for transfections mediated by optimized lipopolymeric formulations as (A) % GFP positive cells and (B) mean intensity of GFP fluorescence (Mean Flu.Intensity). Transfections were performed using pEGFP-C3 pDNA (0.4 µg) in 10% serum. The GFP expression was examined for statistical significance in comparison with BPEI (25 KDa) transfections (*$P < 0.05$ and **$P < 0.01$, Two-tailed Student's t-test).

The lipopolymeric formulation, P8-C6-F1 displayed maximum transfection capability with 10-fold higher luciferase activity at w/w ratio of 4 when compared to BPEI (25 kDa). In flow cytometry experiments P8-C6-F1 showed ~75% GFP positive cells with a mean fluorescence intensity value of ~80, which is much higher than BPEI (25 kDa) and slightly better than Lipofectamine 2000 as well. Expression of GFP was also checked under a fluorescence microscope where the cells treated with polyplexes of P8-C6-F1 appeared to fluoresce significantly higher when compared to BPEI (25 kDa) and slightly better than that of lipofectamine 2000 (Fig. 5). P8-C6-F2 and P8-C6-F3 also exhibited ~6-fold and ~3.5-fold higher transfection efficacies respectively at w/w ratio of 3 than BPEI (25 kDa) and a similar kind of trend was observed in GFP expression too. Formulations containing redox lipopolymers with longer alkyl chain (C11) showed relatively lower transfection efficacies compared to shorter alkyl chain (C6) where P8-C11-F1 showed 4-fold higher transfection efficiency at w/w ratio of 4 than BPEI (25 kDa) (Fig. 3B). Here also the lipopolymers with lowest grafting showed maximum transfection efficiency. P8-C11-F2 exhibited only ~1.8 fold higher transfection at w/w ratio of 3 while P8-C11-F3 displayed lower gene transfection capability than BPEI (25 kDa).

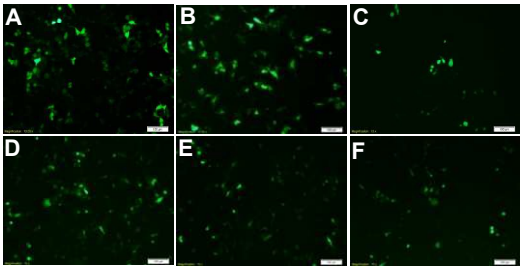

Fig. 5 GFP expression analysis using fluorescence microscopy in HeLa (A-C) and U251 (D-F) cells for the most efficient lipopolymeric formulation, P8-C6-F1 (A and D) in comparison with Lipofectamine 2000 (B and E) and BPEI (25 kDa) (C and F). Transfections were performed using pEGFP-C3 (0.4 µg) pDNA at respective optimized w/w ratios of maximum GFP expression. Scale bar = 100 µm.

We also performed transfection experiments for all the four transfection efficient formulations in the absence of serum (-FBS) and compared the results with those in the presence of serum (+FBS) to look into their serum stability. It was observed that effect of serum was less pronounced on the transfection activity of lipopolyplexes with the lowest degree of alkyl-ferrocene grafting (P8-C6-F1 and P8-C11-F1) (Fig. S10A, ESI†). Additionally, the transfection activity of PEI 25 kDa was significantly impaired in the presence of serum while it was nearly maintained for the efficient lipopolymeric formulations, P8-C6-F1 and P8-C11-F1 (Fig. S10B, ESI†).

Transfection efficacies of all the four efficient redox active formulations P8-C6-F1, P8-C6-F2, P8-C6-F3 and P8-C11-F1 were also checked in U251 (human glioma) cells. A similar trend was observed in transfection capability of all the four formulations except P8-C11-F1 which showed better transfection potential than P8-C6-F2 which was almost close to that of P8-C6-F1 (Fig. S11, ESI†). P8-C6-F1 and P8-C11-F1 showed 3-fold enhancement in luciferase activity than BPEI (25 kDa). P8-C6-F2 showed ~ 2-fold increase in luciferase activity while P8-C6-F3 showed transfection potential almost equal to BPEI (25 kDa).

Influence of the Redox State of Lipopolymers on Gene Transfection

Efficient formulations of the redox polymeric conjugates containing DOPE (P8-C6-F1, P8-C6-F2, P8-C6-F3 and P8-C11-F1) were oxidized and studied for assessing their influence on the gene transfection efficiency at all the five w/w ratios (1:1 to 5:1) in HeLa cells in the presence of serum. Freshly prepared oxidized formulations were used in all the transfection experiments. Oxidation state of ferrocene was found to play a crucial role in mediating an effective gene transfection. Formulations containing oxidized ferrocene showed a drastic reduction in their luciferase activity at all the w/w ratios due to poor transfection (Fig. 6A).

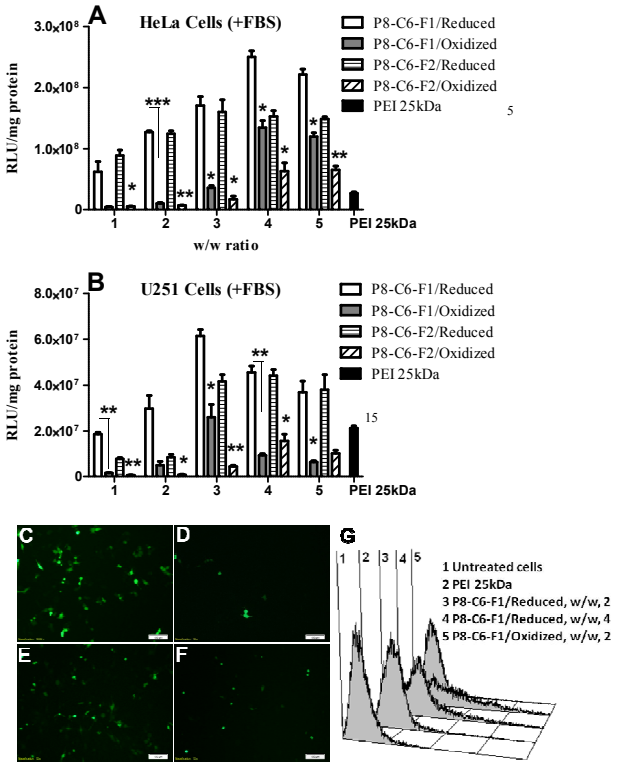

Fig. 6 Comparison of luciferase activities of efficient lipopolymeric formulations (P8-C6-F1 and P8-C6-F2) before and after oxidation of ferrocene in HeLa (A) and U251 cells (B). GFP Expression for transfection of P8-C6-F1 at w/w, 2 in reduced (C and E) and oxidized state (D and F) in HeLa (C and D) and U251 cells (E and F). Flow cytometry histograms of GFP expression in HeLa cells for representative transfections. Transfections were performed using pGL3 control/*p*EGFP-C3 (0.4 μg) *p*DNA in 10% serum. The luciferase activities of oxidized formulations were examined for statistical significance in comparison with that of reduced formulations (**P* < 0.05, ***P* < 0.01 and ****P* < 0.001, Two-tailed Student's t-test).

These results with reduced luciferase activities were supported by fluorescence microscopy and flow cytometry results obtained from GFP expression and there was a good agreement among them (Fig. 6C-6F and Fig. S12, ESI†). A comparative analysis of transfection efficacies of HeLa cells in terms of shifts in flow cytometry histograms have been shown for the most efficient formulation P8-C6-F1 (before and after oxidation of ferrocene) along with BPEI (25kDa) as a positive control (Fig. 6G). Interestingly, the effect of reduction in gene transfection was found to be proportional with the degree of grafting as the reduction in gene transfection was maximum for the lipopolymer, P8-C6-F2 with relatively higher extent of grafting than P8-C6-F1.

It should be emphasized here that these lipopolymeric formulations which are capable of producing efficient gene expression may additionally be used as cytofectins which can provide gene expression in a site specific manner or after a particular time lag for a distinguished cell population under the influence of an external stimulus.[40,47] To explicate the fact we performed the transfection experiment using P8-C6-F1 (w/w, 2) and P8-C6-F2 (w/w, 3) where the oxidized lipopolyplexes were almost inactive and their activities could be resumed significantly after treatment with ascorbic acid (AA) as a reducing agent in cell culture medium during incubation with cells, *i.e.*, extracellular environment.[40] Such treatment led to the resumption in activity of oxidized lipopolyplexes and transfection efficacies (luciferase activities) were almost comparable to that of reduced lipopolyplexes (Fig. 7A). This was corroborated by transfections mediated by pEGFP-C3 plasmid DNA where significantly higher GFP expression was observed for AA treated oxidized lipopolyplexes in comparison with oxidized lipopolyplexes (Fig. 7B and 7C). Therefore such transfection formulations could be extremely beneficial for various biomedical applications where DNA molecules could be delivered to a specific population of cells or in a specific time after externally induced activation.

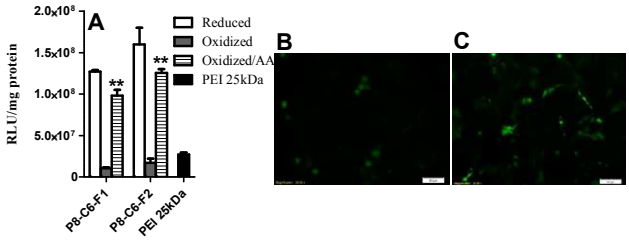

Fig. 7 (A) Luciferase activities of ascorbic acid (AA) treated oxidized lipopolyplexes of P8-C6-F1 (w/w, 2) and P8-C6-F2 (w/w, 3) in HeLa cells in comparison with oxidized (***P* < 0.01) and reduced lipopolyplexes. GFP expression analysis of HeLa cells transfected with oxidized (B) and AA treated-oxidized P8-C6-F1 (C).

Additionally, in U251 cells also, transfection efficacies of the lipopolymers with ferrocene in the oxidized state were significantly much lower than formulations containing reduced ferrocene. In U251 cells, the reduction in transfection efficiency for lipopolymers with oxidized ferrocene was observed to be higher when compared to HeLa cells. Both luciferase activity (Fig. 6B) and GFP expression (Fig. 6E, 6F and Fig. S13, ESI†) were reduced to a significant extent.

To check the transfection of efficient redox lipopolymer before and after oxidation at the level of *p*DNA intracellular delivery, confocal microscopy was undertaken. HeLa cells were transfected with Cy-5 labelled *p*DNA with an incubation period of 4 h.[57] Interestingly, the amount of *p*DNA was significantly higher in HeLa cells transfected with lipopolymer (w/w, 2) in the reduced state of ferrocene (Fig. 8). This further proved the importance of these systems to be used as redox switchable gene transfection vectors as discussed in the preceding section. Taking together all the observations, it could be emphasized here that the lipopolymers showed distinct transfection activities under the influence of redox state of ferrocene and this phenomenon could thus be quite useful for transfections that need a spatial or temporal gene expression in an efficient order.

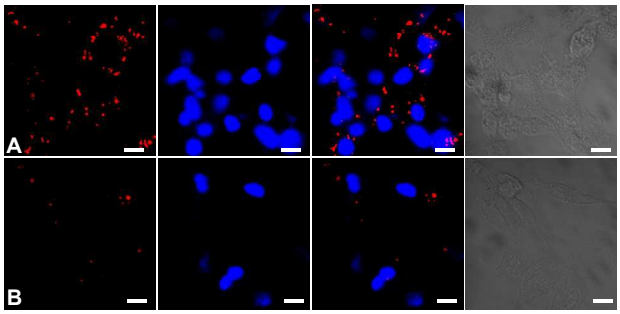

Fig. 8 Representative confocal microscopy images of HeLa cells transfected with P8-C6-F1/Cy5-labelled *p*DNA (w/w, 2) in the reduced (A) and oxidized (B) state of ferrocene. Panels A and B represent (left to right) *p*DNA fluorescence, Hoechst 33342 stained nuclei, overlay of previous two microscopic images and bright field images. Samples were processed after 4 h of lipopolyplex treatment. Scale bar = 10 μm.

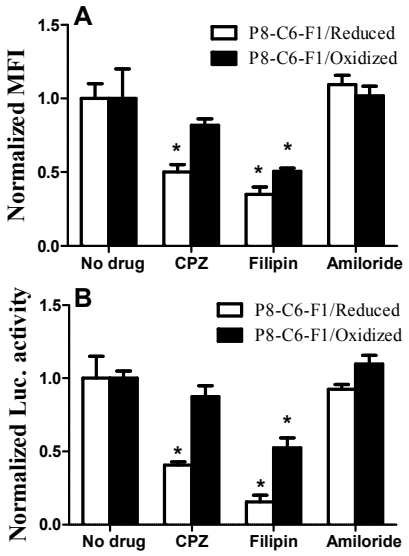

Fig. 9 Effect of endocytosis inhibitors on cellular internalization of Cy5-labelled *p*DNA (A) and subsequent gene expression (luciferase activity) (B) mediated by the efficient P8-C6-F1 lipopolymer (reduced and oxidized). HeLa cells were pretreated with chlorpromazine, CPZ (5 μg/ml) or filipin (1 μg/ml) or amiloride (25 μg/ml). The observations were statistically significant in comparison with untreated controls (*P < 0.05, Two-tailed Student's t-test).

Cellular Uptake Studies

We also undertook experiments to understand the cellular uptake of these redox-active lipopolyplexes in representative HeLa cells. The uptake of lipopolyplexes containing Cy5-labelled *p*DNA and gene transfection capabilities (Luciferase activities) were assessed in the presence of endocytosis inhibitors, chlorpromazine, CPZ (clathrin-mediated), filipin (caveolae-mediated) and amiloride (macropinocytosis).[58-60] HeLa cells which were pre-treated with the inhibitors, CPZ and filipin showed a diminished uptake of reduced as well as oxidized lipopolyplexes. The diminished cellular uptake was much more significant in the case of the reduced lipopolyplexes in both inhibitors treatment when compared to the oxidized lipopolyplexes in filipin pre-treatment (Fig. 9A). This revealed that the reduced lipopolyplexes were internalized using both clathrin and caveolae mediated pathways. However, oxidized lipopolyplexes mainly entered through caveolae mediated pathway, which might be due to their relatively larger sizes.[59] While, amiloride pretreatment had no effect on cellular internalization of the lipopolyplexes. The gene transfection mediated by reduced lipopolyplexes was mitigated significantly in the presence of CPZ and filipin inhibitors, latter being more prominent than CPZ. On the other hand, gene transfection mediated by oxidized lipopolyplexes was impaired only with filipin (Fig. 9B). However, amiloride treatment did not show any reduction in gene expression levels. This suggests that the gene expression mediated by the reduced lipopolyplexes was contributed from both clathrin and caveolae mediated pathways while it was caveolae mediated pathway for the oxidized lipopolyplexes. In contrast to the most of the lipopolymeric formulations, reduced lipopolymers here, contribute significantly to gene transfection via clathrin-mediated pathway and this might be attributed to the presence of DOPE in formulations which destabilizes the endosomal membrane.[61]

Cytotoxicity Assay

Cell viability of lipopolyplexes of each of the efficient redox lipopolymeric conjugates was also assayed as it is one of the important obstacles for the application of non-viral gene delivery vectors.[62-64] Cytotoxicity experiments were performed at all w/w ratios undertaken in transfection experiments for all the four efficient formulations in both HeLa and U251 cells using MTT assay. Lipopolyplexes made up of the efficient formulations with shorter alkyl chain (C6) appeared to be slightly toxic than the one efficient with longer alkyl chain (C11). Here the oxidized ferrocene containing lipopolyplexes did not seem to impart any obvious toxicity to both the cell lines studied. BPEI (25 kDa) was used as a positive control at optimized w/w ratio of 2 where transfection levels were maximum with no significant toxicity. However, there was a significant difference in cell viabilities with respect to the commercial formulation lipofectamine 2000. Lipoplexes made up of Lipofectamine 2000 showed almost 60% cell viabilities in both the cell lines which was lower than the cell viabilities shown by the lipopolyplexes here (>80%). Cell viabilities of all efficient formulations at their w/w ratio of maximum transfection in HeLa (Fig. 10A) and U251 cells (Fig. 10B) are shown in comparison with BPEI (25 kDa) and Lipofectamine 2000.

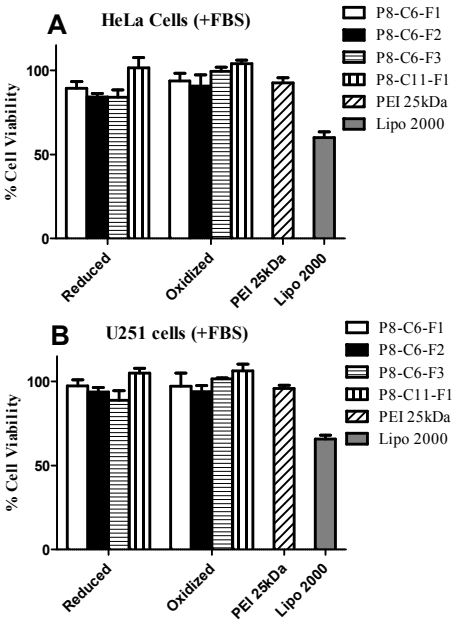

Fig. 10 Cytotoxicity profile of lipopolyplexes derived from different redox-active lipopolymers in HeLa cells (A) and U251 cells (B). Cell viabilities were assayed following actual transfection conditions while using BPEI (25 kDa) and lipofectamine 2000 as controls. Each experiment contained triplicates of every single lipopolyplex treatment and results shown are based on at least three such independent experiments.

Conclusions

A number of ferrocene based redox-active polymers were synthesized using BPEI (800 Da) and suitably crafted using ω-bromo-alkyl ferrocenes via *N*-alkylation. Ferrocene moiety was covalently tethered away from the polymer backbone by two different alkanediyl spacers, *viz*. 6 and 11. The degree of substitution of each long chained ferrocene was varied to give lipopolymers of different hydrophobicity and variable density of ferrocene function. The aggregation properties of each lipopolymer and their co-liposomes with DOPE, were investigated in detail using a number of physical methods such as, TEM, AFM, DLS and zeta potential measurements. There was a significant impact of the oxidation state of ferrocene which manifested as an increase in the size and zeta potential of the redox lipopolymeric aggregates. Optimized lipopolymeric formulations showed improved gene transfection efficacies than BPEI (25 KDa) and Lipofectamine 2000 in the presence of 10% serum environment as evidenced from both flow cytometry and fluorescence microscopic studies. Transfection efficiency of these redox-active lipopolymers was thus strongly dictated by the oxidation state of ferrocene. Gene transfection capabilities of optimized lipopolymer/DOPE formulations reduced drastically upon oxidation of ferrocene which implies that this phenomenon could be useful for spatial and temporal control of gene expression under the influence of external stimuli. Endocytosis inhibition experiments revealed that the gene expression mediated by reduced lipopolymers was due to both clathrin and caveolae mediated pathways while it was only caveolae mediated pathway in case of the oxidized formulations. The lipopolymers did not exhibit any obvious toxicity under the concentrations used for the transfection experiments. Therefore, such ferrocene functionalized BPEIs with improved transfection levels much above BPEI (25 KDa) should be attractive gene transfer reagents for practical use.

Acknowledgements

This work was financially supported by the J. C. Bose Fellowship (S.B.) of the DST, Government of India, New Delhi, India.

Notes and references

[a]*Department of Organic Chemistry, Indian Institute of Science, Bangalore, 560012, India. Fax: +91-80-23600529; Tel: +91-8022932664; E-mail: sb@orgchem.iisc.ernet.in*
[b]*Department of Molecular Reproduction Development and Genetics, Indian Institute of Science, Bangalore, 560012, India. E-mail: paturu@mrdg.iisc.ernet.in*
[c]*Chemical Biology Unit, JNCASR, Bangalore 560 064, India.*

† Electronic Supplementary Information (ESI) available: IR, ^{1}H-NMR, ^{13}C-NMR and ESI-MS of lipopolymer, P8-C6-F1; UV-Vis spectra of P8-C6-F1; TEM of lipopolymers alone and co-liposomes; DLS plots; Luciferase activities of neat lipopolymers; GFP expression analysis for reduced and oxidized formulations. See DOI: 10.1039/b000000x/
‡ These authors contributed equally to this work.

1. S. Bhattacharya and A. Bajaj, *Chem. Commun*., 2009, **11**, 4632-4656.
2. D. J. Glover, H. J. Lipps and D.A. Jans, *Nat. Rev. Genet.*, 2005, **6**, 299-310.
3. A. Bajaj, P. Kondaiah and S. Bhattacharya, *Biomacromolecules*, 2008, **9**, 991-999.
4. T. G. Park, J. H. Jeong and S. W. Kim, *Adv. Drug Delivery Rev.*, 2006, **58**, 467-486.
5. D. Putnam, *Nat. Mater.*, 2006, **5**, 439-451.
6. A. V. Kabanov, *Pharm. Sci. Tech. Today*, 1999, **2**, 365-372.
7. R. Kircheis, L. Wightman and E. Wagner, *Adv. Drug Delivery Rev.* 2001, **53**, 341-358.
8. M. Jäger, S. Schubert, S. Ochrimenko, D. Fischer and U. S. Schubert, *Chem. Soc. Rev.*, 2012, **41**, 4755-4767.
9. G. F. Lemkine and B. A. Demeneix, *Curr. Opin. Mol. Ther.*, 2001, **3**, 178-182.
10. S. Mao, W. Sun and T. Kissel, *Adv. Drug Deliv. Rev.*, 2010, **62**, 12-27.
11. O. Boussif, F. Lezoualch, M. A. Zanta, M. D. Mergny, D. Scherman, B. Demeneix and J. P. Behr, *Proc. Natl. Acad. Sci., U.S.A.*, 1995, **92**, 7297-7301.
12. D. Fischer, T. Bieber, Y. Li, H. P. Elsasser and T. Kissel, *Pharm. Res.*, 1999, **16**, 1273-1279.
13. S. M. Moghimi, P. Symonds, J. C. Murray, A. C. Hunter, G. Debska and A. Szewczyk, *Mol. Ther.*, 2005, **11**, 990-995.
14. W. T. Godbey, K. K. Wu and A. G. Mikos, *J. Biomed. Mater.Res.*, 1999, **45**, 268-275.
15. H. L. Jiang, Y. K. Kim, R. Arote, J. W. Nah, M. H. Cho, Y. J. Choi, T. Akaike and C. S. Cho, *J. Controlled Release*, 2007, **117**, 273-280.
16. Y. X. Sun, X. Wang, S. X. Cheng, X. Z. Zhang and R. X. Zhuo, *J. Controlled Release*, 2008, **128**, 171-178.
17. V. Russ, H. Elfberg, C. Thoma, J. Kloeckner, M. Ogris and E. Wagner, *Gene Ther.*, 2008, **15**, 18-29.
18. H. Petersen, T. Merdan, F. Kunath, D. Fischer and T. Kissel, *Bioconjugate Chem.*, 2002, **13**, 812-821.
19. M. Thomas, Q. Ge, J. J. Lu, J. Z. Chen and A. M. Klibanov, *Pharm. Res.*, 2005, **22**, 373-380.
20. S. S. Diebold, M. Kursa, E. Wagner, M. Cotten and M. Zenke, *Proc. Natl. Acad. Sci. U.S.A.*, 1999, **274**, 19087-19094.
21. M. Neu, D. Fischer and T. Kissel, *J. Gene Med.*, 2005, **7**, 992-1009.
22. Z. Liu, Z. Zhang, C. Zhou and Y. Jiao, *Prog. Polym. Sci.*, 2010, **35**, 1144-1162.

23. V. Incani, A. Lavasanifarab and H. Uludag, *Soft Matter*, 2010, **6**, 2124-2138.
24. A. Neamnark, O. Suwantong, R. K. C. Bahadur, C. Y. M. Hsu, P. Supaphol and H. Uludag, *Mol. Pharmaceutics*, 2009, **6**, 1798-1815.
25. M. Thomas and A. M. Klibanov, *Proc. Natl. Acad. Sci., U.S.A.*, 2002, **99**, 14640-14645.
26. S. O. Han, R. I. Mahato and S. W. Kim, *Bioconjugate Chem.*, 2001, **12**, 337-345.
27. D. A. Wang, A. S. Narang, M. Kotb, A.O. Gaber, D.D. Miller, S.W. Kim and R.I. Mahato, *Biomacromolecules*, 2002, **3**, 1197-1207.
28. A. Bajaj, P. Kondaiah and S. Bhattacharya, *Bioconjugate Chem.*, 2008, **19**, 1640-1651.
29. Q. Peng, F. J. Chen, Z. L. Zhong and R. X. Zhuo, *Chem. Commun.*, 2010, **46**, 5888-5890.
30. A. V. Kabanov, P. Lemieux, S. Vinogradov and V. Alakhov, *Adv. Drug. Delivery Rev.*, 2002, **54**, 223-233.
31. J. Du and R. K. O'Reilly, *Soft Matter*, 2009, **5**, 3544-3561.
32. P. Schattling, F. D. Jochum and P. Theato, *Polym. Chem.*, 2014, **5**, 25-36.
33. M. Huo, J. Yuan, L. Taob and Y. Wei, *Polym. Chem.*, 2014, **5**, 1519-1528.
34. S. Mura, J. Nicolas and P. Couvreur, *Nat. Mater.*, 2013, **12**, 991-1003.
35. A. Bajaj, P. Kondaiah and S. Bhattacharya, *J. Med. Chem.*, 2008**, 51**, 2533-2540.
36. D. Janczewski, J. Song, E. Csanyi, L. Kiss, P. Blazso, R. L. Katona, M. A. Deli, G. Gros, J. Xua and G. J. Vancso, *J. Mater. Chem.*, 2012, **22**, 6429-6435.
37. J. Bigot, B. Charleux, G. Cooke, F. Delattre, D. Fournier, J. Lyskawa, L. Sambe, F. Stoffelbach and P. Woisel, *J. Am. Chem. Soc.*, 2010, **132**, 10796-10801.
38. M. Subramanian, S. K. Mandal, and S. Bhattacharya, *Langmuir*, 1997, **13**, 153-160.
39. N. L. Abbott, C. M. Jewell, M. E. Hays, Y. Kondo and D. M. Lynn, *J. Am. Chem. Soc.*, 2005, **127**, 11576-11577.
40. B. S. Aytar, J. P. E. Muller, S. Golan, S. Hata, H. Takahashi, Y. Kondo, Y. Talmon, N.L. Abbott and D.M. Lynn, *J. Controlled Release*, 2012, **157**, 249-259.
41. Y. J. Ma, W. F. Dong, M. A. Hempenius; H. Moehwald and G. J. Vancso, *Nat. Mater.*, 2006, **5**, 724-729.
42. Q. A. Yan, J. Y. Yuan, Z. N. Cai, Y. Xin, Y. Kang and Y. W. Yin, *J. Am. Chem. Soc.*, 2010, **132**, 9268-9270.
43. S. A. Merchant, T. O. Tran, M. T. Meredith, T. C. Cline, D. T. Glatzhofer and D. W. Schmidtke, *Langmuir*, 2009, **25**, 7736-7742.
44. M. T. Meredith, D.Y. Kao, D. Hickey, D. W. Schmidtke and D. T. Glatzhofer, *J. Electrochem. Soc.*, 2011, **158**, B166-B174.
45. J. K. Sun, K. F. Ren, L. Z. Zhu and J. Ji, *Colloids Surf. B: Biointerfaces*, 2013, **112**, 67-73.
46. S. Bhattacharya and A. Bajaj, *Biochim. Biophys. Acta*, 2008, **1778**, 2225-2233.
47. B. S. Aytar, J. P. E. Muller, Y. Kondo, N.L. Abbott and D.M. Lynn, *ACS Appl. Mater. Interfaces*, 2013, **5**, 8283-8288.
48. K. C. Majumdar, S. Chakravorty, N. Pal and R. K. Sinha, *Tetrahedron*, 2009, **65**, 7998-8006.
49. Y. Han, K. Cheng, K. A. Simon, Y. Lan, P. Sejwal and Y. Y. Luk, *J. Am. Chem. Soc.*, 2006, **128**, 13913-13920.
50. S. A. Merchant, M. T. Meredith, T. O. Tran, D. B. Brunski, M. B. Johnson, D. T. Glatzhofer and D. W. Schmidtke *J. Phys. Chem. C*, 2010, **114**, 11627-11634.
51. A. V. Delgado, in *Interfacial Electrokinetics and Electrophoresis*, Marcel Dekker, New York 2002, Vol. 106.
52. M. Muñoz-Úbeda, S. K. Misra, A. L. Barrán-Berdón, C. Aicart-Ramos, M. B. Sierra, J. Biswas, P. Kondaiah, E. Junquera, S. Bhattacharya and E. Aicart, *J. Am. Chem. Soc.*, 2011, **133**, 18014-18017.
53. A. Bajaj, P. Kondaiah and S. Bhattacharya, *Bioconjugate Chem.*, 2007, **18**, 1537-1546.
54. M. Muñoz-Ubeda, S. K. Misra, A. L. B. Berdon, S. Datta, C. A. Ramos, P. C. Hartmann, P. Kondaiah, E. Junquera, S. Bhattacharya and E. Aicart, *Biomacromolecules*, 2012, **13**, 3926-3937.
55. I. Perevyazko, A. Vollrath, S. Hornig, G. M. Pavlov and U. S. Schubert, *J. Polym. Sci., Part A: Polym. Chem.*, 2010, **48**, 3924-3931.
56. N. Oku, Y. Yamazaki, M. Matsuura, M. Sugiyama, M. Hasegawa and M. Nango, *Adv. Drug Delivery Rev.*, 2001, **52**, 209-218.
57. M. Zheng, Y. Zhong, F. Meng, R. Peng and Z. Zhong, *Mol. Pharmaceutics*, 2011, **8**, 2434-2443.
58. J. Rejman, A. Bragonzi and M. Conese, *Mol. Ther.*, 2005, **12**, 468-474.
59. K. V. Gersdorff, N. N. Sanders, R. Vandenbroucke, S. C. D. Smedt, E. Wagner and M. Ogris, *Mol. Ther.*, 2006, **14**, 745-753.
60. J. Shi, J. G. Schellinger, R. N. Johnson, J. L. Choi, B. Chou, E. L. Anghel and S. H. Pun, *Biomacromolecules*, 2013, **14**, 1961-1970.
61. I. A. Khalil, K. Kogure, H. Akita and H. Harashima, *Pharmacol. Rev.*, 2006, **58**, 32-45.
62. H. Lv, S. Zhang, B. Wang, S. Cui and J. Yan, *J. Controlled Release*, 2006, **114**, 100-109.
63. D. W. Pack, A. S. Hoffman, S. Pun and P. S. Stayton, *Nature Rev. Drug Discov.*, 2005, **4**, 581-593.
64. S. K. Misra, P. Kondaiah, S. Bhattacharya, D. Boturyn and P. Dumy, *J. Mater. Chem. B*, 2014, **2**, 5758-5767.

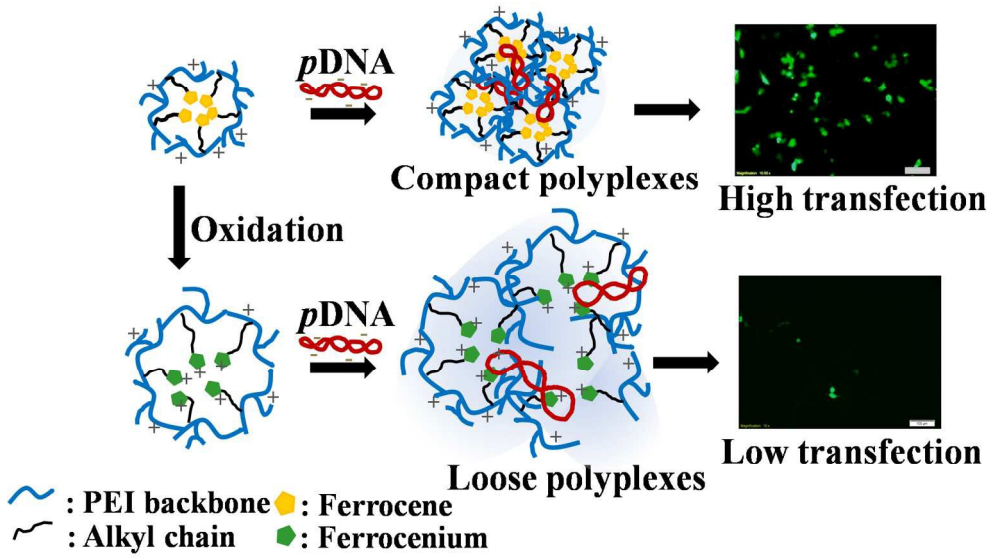

314x178mm (150 x 150 DPI)